

# 1 **Operation stability analysis of district heating substation from the** 2 **control perspective**

3 Yaran Wang <sup>a,b</sup>, Shijun You <sup>a,b</sup>, Huan Zhang <sup>a,b</sup>, Xuejing Zheng <sup>a,\*</sup>, Shen Wei <sup>c</sup>,  
4 Qingwei Miao <sup>a</sup>, Wandong Zheng <sup>a</sup>  
5

6 <sup>a</sup> *School of Environmental Science and Engineering, Tianjin University, Tianjin 300350, PR*  
7 *China*

8 <sup>b</sup> *Key Laboratory of Efficient Utilization of Low and Medium Grade Energy, MOE, Tianjin*  
9 *University, Tianjin 300350, PR China*

10 <sup>c</sup> *Faculty of Engineering and Environment, Northumbria University, Newcastle upon Tyne*  
11 *NE1 8ST, UK*

12 <sup>\*</sup> *Corresponding author. Tel.: +086013512419172; fax: +8602227400832. E-mail addresses:*  
13 *zhengxuejing@tju.edu.cn*  
14

## 15 **Highlights**

- 16 ✓ Oscillatory of flow rate observed in district heating substation
- 17 ✓ Mathematical model describing thermal dynamics of heating substation
- 18 ✓ Control theory based criterion for operation stability of heating substation
- 19 ✓ Conditions that leads to operation instability of district heating substation
- 20 ✓ Controller tuning of the plate heat exchanger to ensure robust stability

## 22 **Keywords**

23 District heating substation; Mathematical model; Operation instability; Stability  
24 analysis; Feedback control; Plate heat exchanger  
25

## 26 **Abstract**

27 Since the heating substation plays a key role in transferring the thermal energy

28 from the primary network to the secondary network and controlling the heat output of  
29 district heating system to meet the thermal load, high operation performance of  
30 heating substation is essential for energy conservation, cost saving and emission  
31 reduction. The dynamic operation stability of heating substation is a very important  
32 dynamic characteristic of heating substation and largely affects the operation  
33 efficiency of district heating system. The operation instability of heating substation  
34 mainly manifest as flow rate and pressure oscillations, which will deteriorate the  
35 network hydraulic condition, break the network thermal balance, reduce the consumer  
36 comfort and increase the energy cost of the pumping system. Since heating  
37 substations will easily operate unstably under some conditions, this paper presents a  
38 theoretical method to analyze the stability and retune the feedback controller for  
39 operation stability of heating substation. Mathematical model of the plate heat  
40 exchanger was established and the feedback control theory was adopted to study the  
41 operation stability of heating substation. Based on the mathematical model and  
42 feedback control theory, a stability criterion was proposed for analyzing the operation  
43 stability of district heating substation effectively. The dynamic model of plate heat  
44 exchanger was validated with measured data. Simulation results show that controller  
45 tuned at certain operating condition can't ensure operation stability of heating  
46 substation, when operating condition varies in large range. The stability analysis  
47 method proposed in this paper can be applied to analyzing the operation stability and  
48 tuning the controller of heating substation to enhance the operation stability.

49

Nomenclature	
$A$	matrix of state space model
$b$	width of the plate heat exchanger flow channel (m)
$B_1, B_2, B_3, B_4$	matrices of linearized state space model
$C$	matrix of linearized state space model
$c_p$	specific heat capacity of water (W/kg · K)
$C_v$	flow capacity of control valve
$C_{Nu}$	the empirical parameter
$d$	distance between neighboring plates (m)
$D$	hydraulic diameter (m)
$G(s), G_{d,1}(s), G_{d,2}(s), G_{d,3}(s), G_{d,4}(s)$	transfer function of linearized plate heat exchanger model
$i$	$\sqrt{-1}$
$k$	overall heat transfer coefficient (W/m <sup>2</sup> · K)
$K$	transfer function of controller
$k_c$	controller gain
$k_v$	valve gain
$l$	length of flow channel
$L(i\omega)$	loop transfer function
$M$	number of flow channels in each side
$N$	number of the control volumes in a flow channel
$n_1, n_2$	the empirical parameter
$Nu$	the Nusselt number
$Pr$	the Prantl number
$q$	volume flow rate (m <sup>3</sup> /s)
$R$	the rangeability of the valve
$Re$	the Reynolds number
$s$	the Laplace variable
$t$	time (s)
$T$	temperature (°C)
$x$	coordinate along the flow channel (m)
$z$	controller zero
$\lambda$	heat conductivity coefficient (W/m <sup>2</sup> · K)
$\mu$	the dynamic viscosity
$\rho$	density of the water (kg/m <sup>3</sup> )
$\tau$	time delay of temperature sensor (s)
$\delta$	small deviation & increment symbol of variable
$\omega$	frequency (rad/s)

Nomenclature	
$\Delta x$	length of a control volume (m)
Subscripts	
$h$	high temperature side
$in$	inlet
$l$	low temperature side
$out$	outlet

50

## 51 **1. Introduction**

52 In China, The total energy consumption of district heating systems in northern  
53 areas covers 24% of the total energy cost of building energy systems [1]. Therefore,  
54 improving the operation efficiency of district heating system is important to reducing  
55 energy cost and enhancing room comfort. In large scale district heating systems, the  
56 heating substations are the terminals, which control the heat outputs to the secondary  
57 networks. Efficient regulation of the district heating network relies on effective  
58 operation and control of the heating substation.

59 There have been numerous researches on improvement of heating substation  
60 efficiency by applying new control strategy. Gustafsson et al. [2] developed a new  
61 control approach for indirectly connected district heating substations based on a  
62 physical model, which maximizes the  $\Delta T$  of the district heating network. They also  
63 verified the control method experimentally through implementation of the control  
64 method in a real district heating substation; the results confirms that it is possible to  
65 control the radiator system based on the primary supply temperature while  
66 maintaining comfort; however, conclusions regarding improvements in  $\Delta T$  were hard  
67 to distinguish [3]. Since high return temperature will lead to large amount of overall

68 distribution energy cost, the temperature difference faults can be detected and  
69 eliminated by using fault detection approaches. Gadd and Werner [4, 5] presented a  
70 fault detection based method to achieve low return temperatures in district heating  
71 substations.

72 Modeling the heating substation is important to analyzing and evaluating the  
73 operation performance of heating substation. Brand et al. [6] developed a numerical  
74 model for heating substation, which takes into consideration the effect of service  
75 pipes. With this model, they studied the effects of service pipe on waiting time for  
76 DHW, heat loss, and overall cost. Brand et al. [7] also used the commercial software  
77 IDA-ICE and Termis to model and analyze various solutions for controlling the  
78 redirected bypass flow and evaluated their performance and the effect on the DH  
79 network in heating substation. Kuosa [8] developed a numerical model for a district  
80 heating system with ring network, with which the variations of flow rates, pressure  
81 losses and overall heat transfer coefficients of plate heat exchanger in heating  
82 substation were simulated and analyzed on selected days. Dobos and Abonyi [9]  
83 developed the nonlinear dynamic model of the district heating network including the  
84 heat exchanger in heating substations, heat production units and pipelines to study the  
85 nonlinear model predictive control of district heating network.

86 Since plate heat exchanger is the core component of heating substation,  
87 mathematical modeling and control performance analysis of plate heat exchanger is  
88 important to improve the operation efficiency of district heating substation. Feedback  
89 control analysis and design of plate heat exchangers have been paid attentions.

90 Al-Dawery [10] established a first order model with time delay to suggest the  
91 transient responses of a plate heat exchanger, and a fuzzy logic controller of the plate  
92 heat exchanger was designed to achieve less settling time and oscillatory behavior.  
93 Michel and Kugi [11] developed a control strategy without knowledge of the heat  
94 transfer of plate heat exchanger based on controlling the total thermal energy stored in  
95 the heat exchanger and a Kalman Filter to estimate the states.

96       However there were few studies concerning the dynamic operation stability of  
97 heating substation, which is a very important dynamic characteristic for heating  
98 substation and largely affects the operation efficiency of district heating system. The  
99 operation instability of heating substation mainly manifest as flow rate and pressure  
100 oscillations, which will deteriorate the network hydraulic condition, break the network  
101 thermal balance, reduce the consumer comfort and increase the energy cost of the  
102 pumping system. Since heating substations will easily operate unstably under some  
103 conditions, this paper presents a theoretical method to analyze the stability and retune  
104 the feedback controller for operation stability of heating substation. The theoretical  
105 method presented in this paper mainly utilized the techniques developed in feedback  
106 control theory [12]. The feedback control theory has been effectively applied to  
107 analyze the operation stability and elimination of oscillations in a central heating  
108 system using pump control [13]. Tahersima et al. utilized the feedback control theory  
109 to study the stability performance and developed a gain scheduling controller of  
110 radiator heating system in a room [14]. In our previous work, the control oriented  
111 approaches were adopted to establish an accurate low order model of room heating

112 system and propose a two-degrees-of-freedom  $H_\infty$  loop-shaping controller [15].  
113 Research on the operation stability of district heating system focuses on dynamic  
114 variation and fluctuation of flow rates, pressures and temperatures in the district  
115 heating network, which is very important and applicable in improving the operating  
116 efficiency of the district heating network. In this paper, the operation stability of  
117 district heating substation was studied from the control perspective. An analytical tool  
118 was developed to analyzing the operation stability of district heating substation.

119

120

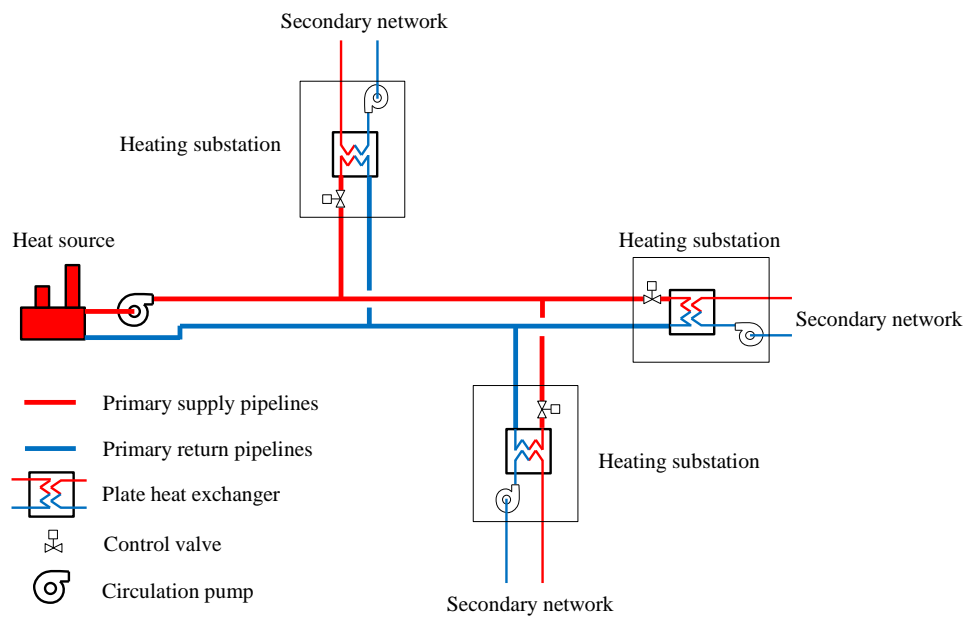
121

## 122 **2. Control levels of district heating system**

123 Fig. 1 shows the schematic of district heating system. The hot water is generated  
124 from the heat source and delivered to the heating substations by the primary  
125 circulation pump along the primary pipelines. The heating substations are usually  
126 located near the center of load regions. The main components of a heating substation  
127 are the plate heat exchanger, primary control valve, secondary circulation pump and  
128 the control system.

129 In order to provide sufficient thermal energy effectively, the district heating  
130 system is usually regulated under three control levels. The first level is named the  
131 centralized control; this level functions at the heat sources, which controls the primary  
132 supply temperature and the pump speed to meet the total heating load variations of the  
133 network. The second level is called the local control; this level functions at each

134 heating substation, which controls the secondary supply temperature and secondary  
 135 pump speed to satisfy the variable heating load of the heat consumers. The secondary  
 136 supply temperature is controlled by adjusting the control valve of the plate heat  
 137 exchanger at the primary side. The third level is personal control; this level functions  
 138 at each radiator, which controls the flow rate of radiator according to the room  
 139 temperature difference between the desired and value to maintain the room air  
 140 temperature around the desired value. In district heating system operation, the three  
 141 control levels work simultaneously to allocate heat to each consumer. Fig. 1 shows the  
 142 control structure of district heating network. As is shown, local control plays a key  
 143 role in controlling the heat output of the primary network.



144

145 Fig. 1. Schematic of district heating system and heating substation

146



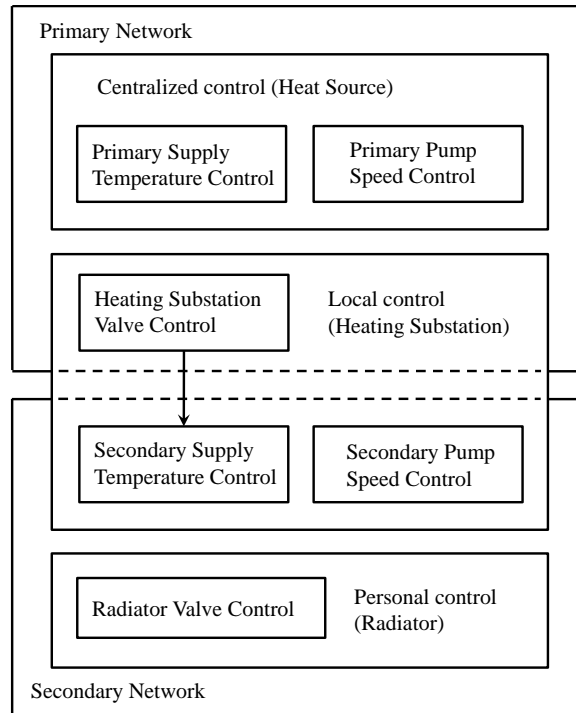


Fig. 2. Control levels of the district heating network.

147

148

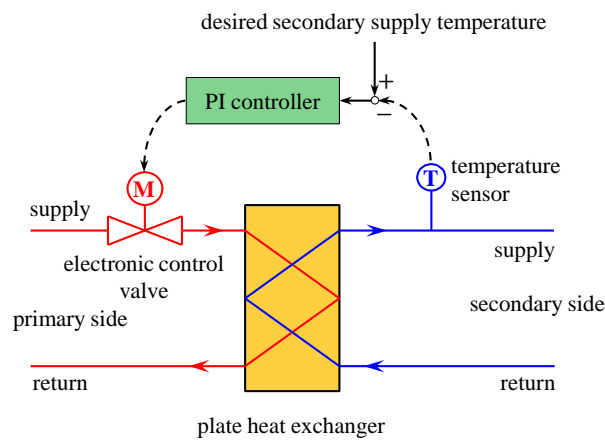
149

150 Fig.3 shows the schematic of the feedback control structure in heating substation,  
 151 which composes the main part of the local control. Efficient operation of the heating  
 152 substation requires the feedback control loop to be stable. However, numerous heating  
 153 substations are working in unstable conditions, and oscillations of flow rate and  
 154 pressure always occur. The instability is resulted from the nonlinearities of valve and  
 155 plate heat exchanger, sensor delay and improperly-tuned controller.

156 Fig.4 shows the measured primary side flow rate, supply temperature and  
 157 outdoor temperature of a district heating substation in Tianjin, China. The secondary  
 158 side of the heating substation is a commercial building with 22 floors. These  
 159 measured data are to illustrate the operation instability of a district heating substation.  
 160 As is shown, oscillation of primary side flow rate occurs when supply temperature is

161 high. Such oscillation may deteriorate the hydraulic condition of the district heating  
 162 network, increase the energy cost of pumping system and reduce the lifetime of  
 163 control valve. In order to investigate the instability analytically and stabilize the  
 164 heating substation with properly-tuned controller, mathematical models of the heat  
 165 exchanger and the feedback controller are established.

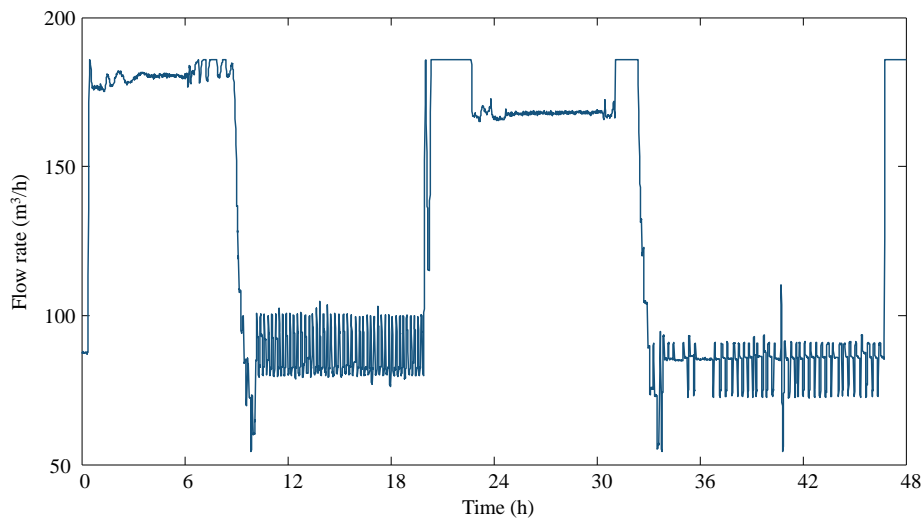
166



167

168 Fig. 3. Schematic of heating substation control system

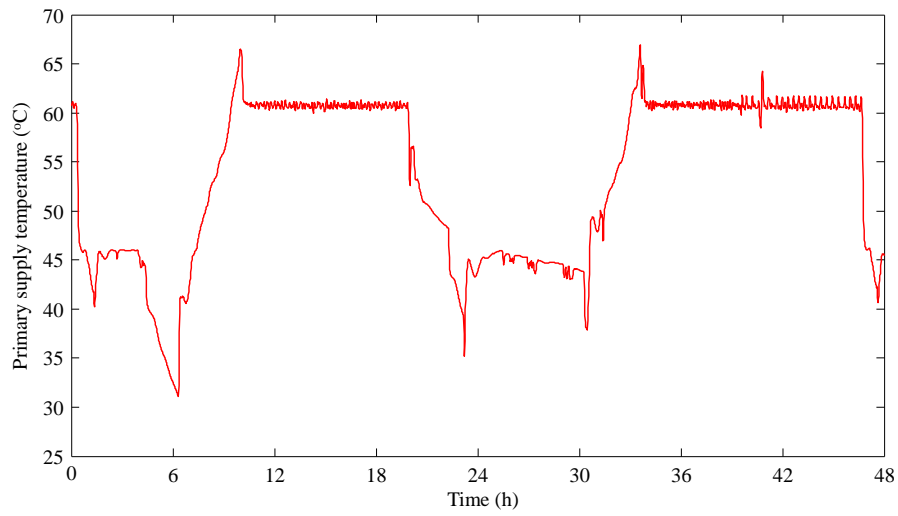
169



170

171 (a)

172

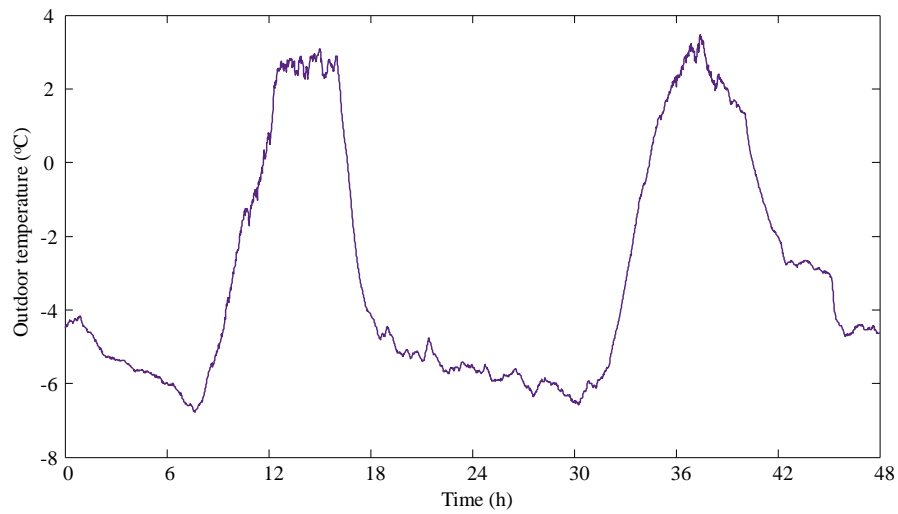


173

174

(b)

175



176

177

(c)

178 Fig.4. Measured primary side data of a heating substation in Tianjin, China. (a) Measured primary

179 side flow rate. (b) Measured primary supply temperature. (c) Measured outdoor temperature.

180

181 **3. Modeling the plate heat exchanger**

182 The thermal dynamics of plate heat exchanger can be described by a pair of  
 183 partial differential equations (PDEs) [11]:

$$184 \quad \frac{\partial T_h}{\partial t} = \frac{q_h}{Mbd} \frac{\partial T_h}{\partial x} + \frac{k}{\rho c_p d} (T_l - T_h) \quad (3)$$

$$185 \quad \frac{\partial T_l}{\partial t} = -\frac{q_l}{Mbd} \frac{\partial T_l}{\partial x} + \frac{k}{\rho c_p d} (T_h - T_l) \quad (4)$$

186 where  $T_h$  and  $T_l$  are the temperature distribution of the high temperature side and  
 187 the low temperature side, respectively.  $M$  is the number of flow channels in each side.  
 188  $b$  is the width of each flow channel.  $d$  is the distance between neighboring plates.  
 189  $q_h$  and  $q_l$  are the flow rates of the high temperature side and low temperature side,  
 190 respectively.  $\rho$  is the water density.  $c_p$  is the specific thermal capacity.  $k$  is the  
 191 overall heat transfer coefficient of the plate heat exchanger, which is the function of  
 192 flow rates of the two sides. Calculation of  $k$  is summarized in Appendix A.

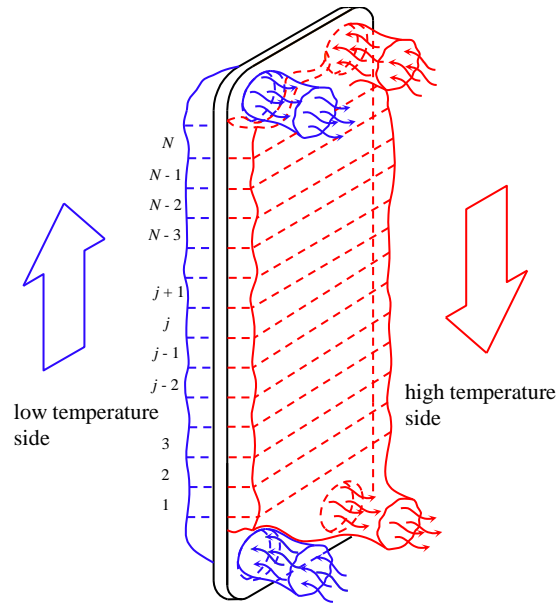
193 The PDE model can be reduced to an ordinary differential equation (ODE)  
 194 model with the finite volume/difference method. Fig. 4 illustrates the finite volume  
 195 division of the plate heat exchanger. The ODE model of plate heat exchanger can be  
 196 derived as:

$$197 \quad \frac{dT_{h,j}}{dt} = \frac{q_h}{Mbd\Delta x} (T_{h,j+1} - T_{h,j}) + \frac{k}{\rho c_p d} (T_{l,j} - T_{h,j}) \quad (5)$$

$$198 \quad \frac{dT_{l,j}}{dt} = -\frac{q_l}{Mbd\Delta x} (T_{l,j} - T_{l,j-1}) + \frac{k}{\rho c_p d} (T_{h,j} - T_{l,j}) \quad (6)$$

199 where  $\Delta x = l/N$ ;  $j = 1, \dots, N$ ;  $l$  is the channel length;  $N$  is the number of volumes  
 200 divided in each channel;  $T_{h,N+1} = T_{h,in}$  and  $T_{l,0} = T_{l,in}$  are the inlet temperatures of  
 201 the high temperature and low temperature sides, respectively;  $T_{h,1} = T_{h,out}$  and  
 202  $T_{l,N} = T_{l,out}$  are the outlet temperatures of the high temperature and low temperature  
 203 sides, respectively.

204



205

206

Fig. 4. Finite volume division of the plate heat exchanger flow channel.

207

208 The feedback control theory based method adopted in this paper generally  
209 includes three steps. The first step is to develop the dynamic model of plate heat  
210 exchanger, control valve and controller. The dynamic model of plate heat exchanger is  
211 a pair of nonlinear ordinary differential equations describing the thermal dynamics of  
212 the heat transfer process between the high temperature and low temperature sides.  
213 Since the models of plate heat exchanger and control valve are nonlinear, they should  
214 be linearized at an equilibrium point for stability analysis of the heating substation  
215 control loop with the feedback control theory. The second step is to do Laplace  
216 transform for the linearized models and derive the loop transfer function of the whole  
217 system  $L(s)$  (transfer function from primary flow rate to secondary supply  
218 temperature) [12]. The third step is to draw the curve of  $L(s)$  on the complex plane  
219 for  $s$  varying along the imaginary axis from 0 to  $i\infty$ . This curve is called the

220 Nyquist curve [12]. The operation stability of heating substation can be judged with  
221 the relation between the Nyquist curve and the point  $(0, -1)$  on the complex plane.  
222 The Nyquist curve method for analyzing stability of dynamic systems named the  
223 Nyquist criterion was developed in 1930s, which has become a core concept and  
224 technique of classical control theory [12]. The Nyquist criterion is very applicable to  
225 practical problems and has been extended to more modern control technique [17].

226 The rest of this paper is organized as follows. The next section illustrates the  
227 control levels of the whole district heating system. The primary flow rate oscillation  
228 was observed from the measured data of a heating substation in Tianjin, China. Then  
229 the nonlinear ordinary differential equation model of plate heat exchanger was derived.  
230 The stability analysis method for heating substation was developed with the linearized  
231 model of heating substation and the Nyquist criterion. The nonlinear plate heat  
232 exchanger model was validated with measured data from the literature. The dynamic  
233 responses and operation stability of a heating substation were studied for application  
234 of the proposed stability analysis method.

235

## 236 **4. Operation stability analysis method**

### 237 *4.1. Model linearization*

238 Dynamic model of plate heat exchanger Eq. (5) and (6) is nonlinear. In order to  
239 analyze the operation stability with the frequency domain method, model linearization  
240 is required [17]. The nonlinear model described by Eq. (5) and (6) can be linearized  
241 into the following linear state space form:

242 
$$\frac{dT}{dt} = AT + B_1q_h + B_2q_l + B_3T_{h,in} + B_4T_{l,in} \quad (7)$$

243 
$$T_{l,out} = CT \quad (8)$$

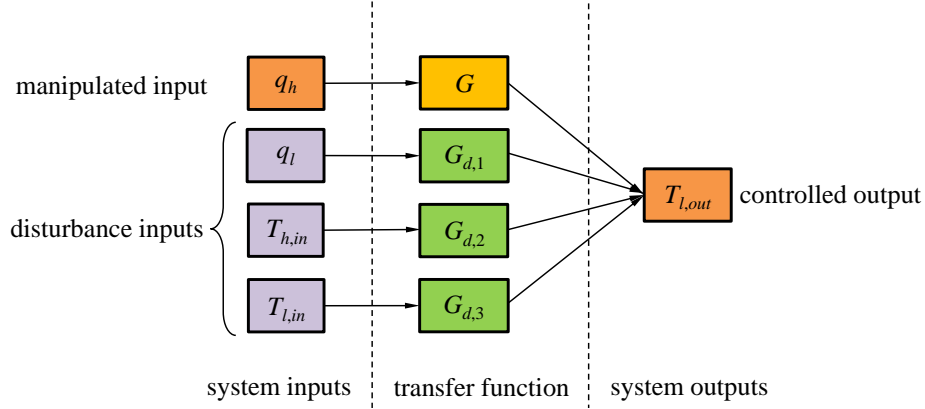
244 where  $T = [T_{h,1} \ T_{h,2} \ \dots \ T_{h,N} \ T_{l,1} \ T_{l,2} \ \dots \ T_{l,N}]^T$ .  $A$ ,  $B_1$ ,  $B_2$ ,  $B_3$ ,  $B_4$   
 245 and  $C$  are constant matrices (details for derivation of the matrices are listed in  
 246 **Appendix A**). Doing Laplace transform to Eq. (7) and (8), the input-output model of  
 247 plate heat exchanger can be written in the following form:

248 
$$T_{l,out} = G(s)q_h + G_{d,1}(s)q_l + G_{d,2}(s)T_{h,in} + G_{d,3}(s)T_{l,in} \quad (9)$$

249 where  $G(s)$ ,  $G_{d,1}(s)$ ,  $G_{d,2}(s)$  and  $G_{d,3}(s)$  are transfer functions, that can be  
 250 calculated with the matrices  $A$ ,  $B_1$ ,  $B_2$ ,  $B_3$ ,  $B_4$  and  $C$  (see **Appendix A**). When  
 251 linearizing a nonlinear system like Eq. (5) and (6), an equilibrium point should be  
 252 specified. The equilibrium point of Eq. (5) and (6) is the solution of the steady state  
 253 Eq. (5) and (6) (of which the time derivatives are made zero), with specified steady  
 254 state inputs:  $q_h$ ,  $q_l$ ,  $T_{h,in}$  and  $T_{l,in}$ . Therefore, with different steady state inputs,  
 255 different equilibrium points can be derived. Since the matrices:  $A$ ,  $B_1$ ,  $B_2$ ,  $B_3$  and  
 256  $B_4$  of the linearized model Eq. (7) and (8) are dependent on the equilibrium point.  
 257 Different selection of equilibrium points will lead to different linearized models.  
 258 However, all of the possible equilibrium points of the nonlinear system (Eq. (5) and  
 259 (6)) lead to a set of linearized models, with which it is sufficient to study the robust  
 260 stability of the nonlinear system [17].

261 The input-output structure of plate heat exchanger is illustrated in Fig. 5. The  
 262 inputs can be divided into two categories: manipulated inputs and disturbance inputs.  
 263 In district heating substation, the secondary supply temperature  $T_{l,o}$  is controlled by

264 adjusting the primary flow rate  $q_h$ . Therefore  $q_h$  is the manipulated input, and the  
 265 primary supply temperature  $T_{h,in}$ , secondary flow rate  $q_l$  and secondary return  
 266 temperature  $T_{l,in}$  are disturbance inputs .



267

268 Fig. 5. Input-output structure of the plate heat exchanger.

269

#### 270 4.2. Models of the controller and valve

271 The PI control law is usually adopted as feedback controller  $K$  in district  
 272 heating substation, and  $K$  can be represented as the Laplace transform form:

$$273 \quad K = k_c \frac{s+z}{s} \quad (10)$$

274 where  $k_c > 0$  is the controller gain and  $z > 0$  is controller zero.

275 The equal percentage valve is usually used in heating substation. The  
 276 characteristic for equal percentage valve is nonlinear. The relation between flow rate  
 277 and valve opening of equal percentage valve can be characterized by the following  
 278 formula [13, 18]:

$$279 \quad q = C_v \sqrt{\Delta p} R^{x-1} \quad (11)$$

280 where  $C_v$  is the flow capacity of the valve;  $R$  is the rangeability of the valve;  $\Delta p$   
 281 is the pressure difference of the valve. Fig. 6 shows the characteristic of an equal

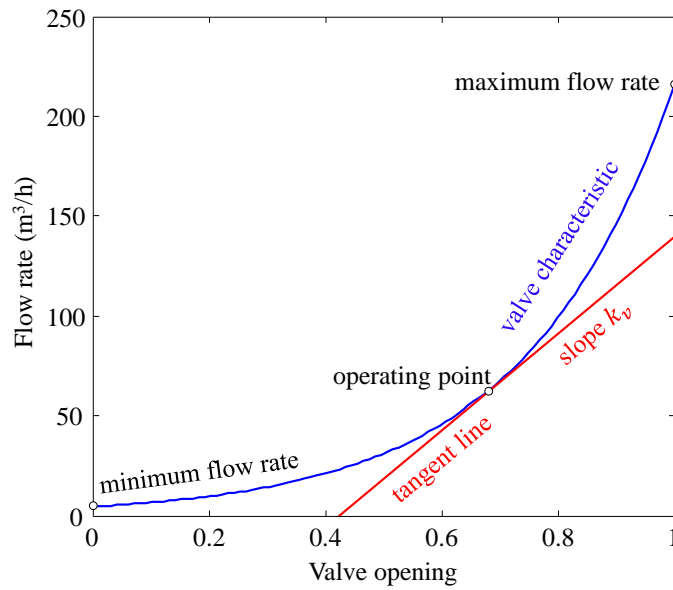


282 percentage valve with  $C_v = 450$ ,  $\Delta p = 0.23\text{atm}$  and  $R = 50$ . Fig. 6 also shows the  
 283 tangent line of valve characteristic line. The slope of the tangent line can be derived  
 284 by:

$$285 \quad k_v = \left( \frac{\partial q}{\partial x} \right)_{x=x_0} \quad (12)$$

286  $x_0$  is the operating point.

287



288

289 Fig. 6. Characteristic of an equal percentage valve.

290

291 The block diagram of heating substation feedback control system can be  
 292 illustrated as Fig. 7. Since the valve characteristic is nonlinear, the valve gain  $k_v$  is  
 293 varying with the operating point  $x_0$  changing. The varying range of valve gain  
 294  $k_{v,min} \leq k_v \leq k_{v,max}$  can be derived from the valve characteristic Eq. (11) and (12)  
 295 as follows.

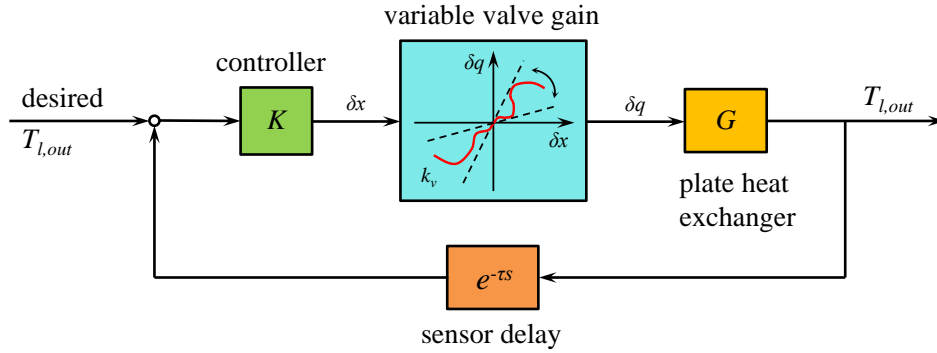
$$296 \quad k_{v,min} = \left( \frac{\partial q}{\partial x} \right)_{x=0} = C_v \sqrt{\Delta p} R^{-1} \ln R$$

297  $k_{v,max} = \left(\frac{\partial q}{\partial x}\right)_{x=1} = C_v\sqrt{\Delta p}\ln R$

298 Therefore, the varying valve gain satisfies:

299  $C_v\sqrt{\Delta p}R^{-1}\ln R < k_v \leq C_v\sqrt{\Delta p}\ln R$  (13)

300



301

302 Fig. 7. Block diagram of heating substation control system.

303

#### 304 4.3. Stability criterion of heating substation

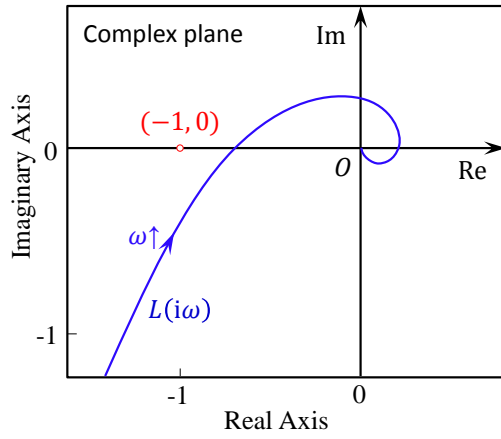
305 According to the feedback control theory [17], the operation stability of feedback  
 306 control system can be judged by the Nyquist stability criterion. If introducing this  
 307 criterion to heating substation system, the operation stability of district heating  
 308 substation can be judged by the following criterion:

309 If the curve of  $L(s) = k_v K(s)G(s)e^{-\tau s}$  ( $s$  is varying along the imaginary axis  
 310 from  $0$  to  $i\infty$ ) encircles or crosses the point  $(-1, 0)$  on the complex plane, the heating  
 311 substation control system will be unstable.

312 Here the complex variable  $s$  can be replaced by the pure imaginary variable  $i\omega$   
 313 with  $0 \leq \omega < +\infty$ , where  $i = \sqrt{-1}$ . Fig. 8 shows three cases of the relation between  
 314 the curve of  $L(i\omega)$  and the point  $(-1, 0)$ . For cases (b) and (c), the heating substation

315 will be unstable.

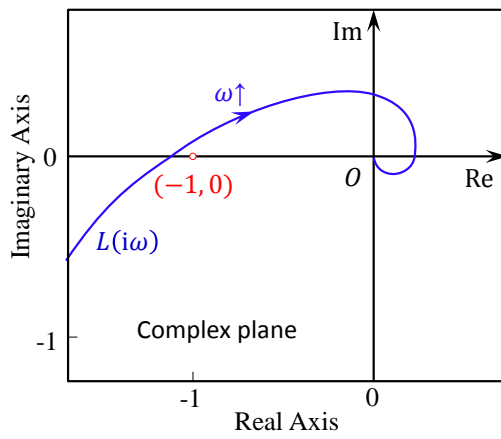
316



317

318

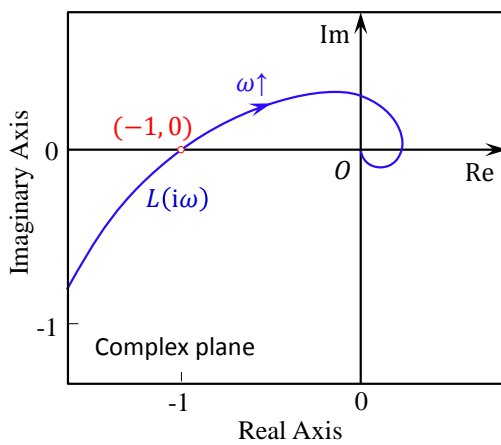
(a)



319

320

(b)



321

322

(c)

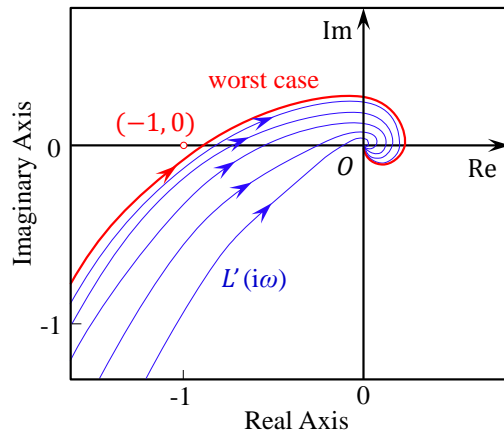
323 Fig. 8. Nyquist plots for operation stability analysis of heating substation. (a) The curve of  $L(i\omega)$   
324 doesn't encircle point  $(-1, 0)$ . (b) The curve of  $L(i\omega)$  encircles point  $(-1, 0)$ . (c) The curve of  
325  $L(i\omega)$  crosses the point  $(-1, 0)$ .

326

327 Since the dynamics of plate heat exchanger is nonlinear, the linearized model  $G$   
328 will be perturbed to  $G'$  ( $G' \neq G$ ), if the operating condition (equilibrium point) is  
329 changed. And the perturbation may lead to instability of the heating substation control  
330 system. According to the proceeding criterion and Fig.8, operation stability of heating  
331 substation will be damaged, if the perturbed system  $G'$  causes the curve of  $L'(i\omega) =$   
332  $k_v'K(i\omega)G'(i\omega)e^{-i\omega\tau}$  to encircle or cross the point  $(-1, 0)$ . The conversion from  
333 stability to instability may happen, when operating condition of plate heat exchanger  
334 in heating substation changes largely. As is observed in Fig. 3, with the primary  
335 supply temperature increasing to a high level, the operation stability of heating  
336 substation will be damaged, and the oscillatory will occur.

337 Therefore, case (a) for a certain operating condition doesn't mean that the  
338 heating substation will be stable for all operating conditions. To ensure robust stability  
339 of heating substation at all conditions, the case (a) should be held for all perturbed  
340 models  $G'$  at any operating conditions. This criterion also indicates that robust  
341 stability for all operating conditions can be ensured with a small loop gain:  $|L(i\omega)|$ ,  
342 which means that if the absolute value of  $L(i\omega)$  is small enough, operation stability  
343 can always be satisfied. This can be intuitively observed from Fig. (8). Fig. 9 shows

344 the Nyquist plots of all possible operating conditions (equilibrium points). As is  
 345 shown if all of these curves do not encircle or cross point  $(-1, 0)$ , the heating  
 346 substation will be stable at all operating conditions. This is equivalent to that the  
 347 worst case Nyquist curve doesn't encircle or cross point  $(-1, 0)$ .  
 348



349

350 Fig. 9. Nyquist plots of all possible operating conditions (equilibrium points).

351

352 With this criterion, the operation stability of heating substation is predictable.  
 353 Besides, for an unstable operation condition of heating substation, this criterion can  
 354 also be used to analyze the key factor which leads to the instability of the heating  
 355 substation and tune the controller to ensure robust stability.

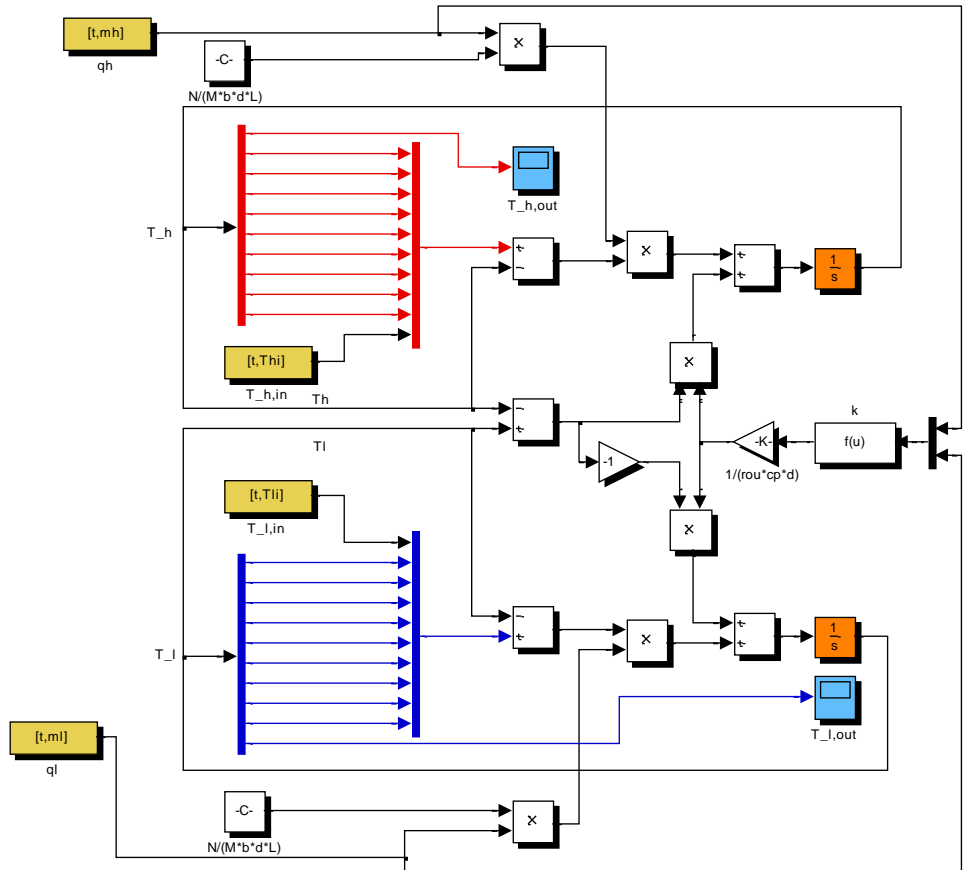
356

## 357 5. Results and discussion

### 358 5.1. Validation of the nonlinear model

359 The nonlinear model of plate heat exchanger described by Eq. (5) and (6) was  
 360 established in Simulink (Fig. 10). In Ref. [16], Michel and Kugi have tested the

361 dynamic operation of plate heat exchanger, and the measured data were used to  
362 validate the dynamic model of plate heat exchanger. If the nonlinear model of plate  
363 heat exchanger described by Eq. (5) and (6) is effective, the model should be able to  
364 predict the dynamic operation in Ref. [16]. The plate heat exchanger parameters and  
365 measured data including the boundary conditions of inlet temperatures and flow rates  
366 in both sides given in Ref. [16] have been used to validate the proposed nonlinear  
367 model described by Eq. (5) and (6). The nonlinear model was validated using the  
368 measured data and plate heat exchanger parameters given in Ref. [16]. The simulated  
369 and measured outlet temperatures  $T_{h,out}$  and  $T_{l,out}$  are shown in Fig. 11, and the  
370 relative errors of  $T_{h,out}$  and  $T_{l,out}$  are shown in Fig.12. Relative errors of the  
371 simulated  $T_{h,out}$  and  $T_{l,out}$  are both varying within  $\pm 8\%$ , which is in a satisfied  
372 range. Therefore, the nonlinear model of the plate heat exchanger Eq. (5) and (6) can  
373 describe the thermal dynamics of the plate heat exchanger with satisfied accuracy.

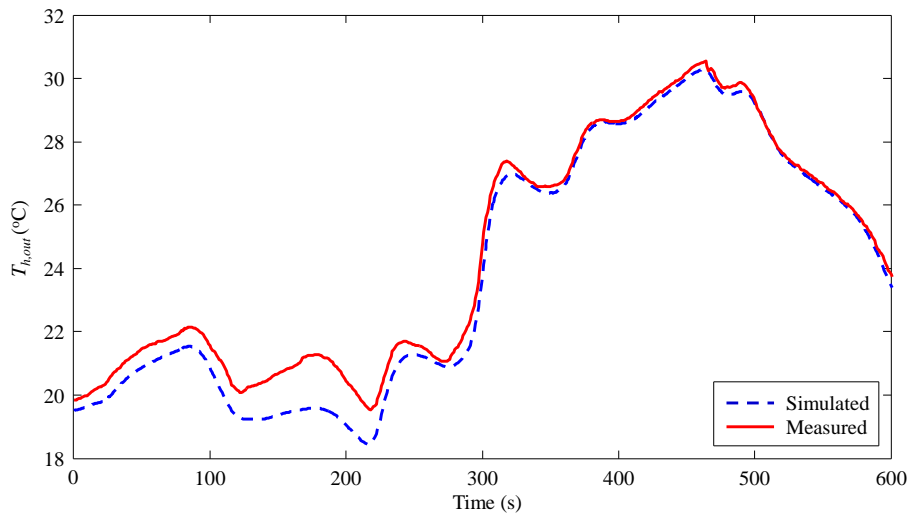


374

375

Fig. 10. Simulink model of the nonlinear plate heat exchanger model Eq. (5) and (6).

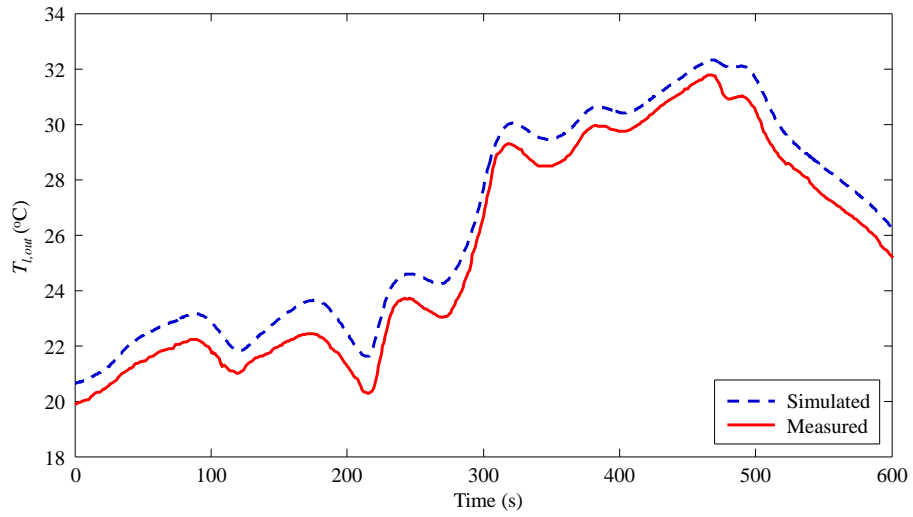
376



377

378

(a)

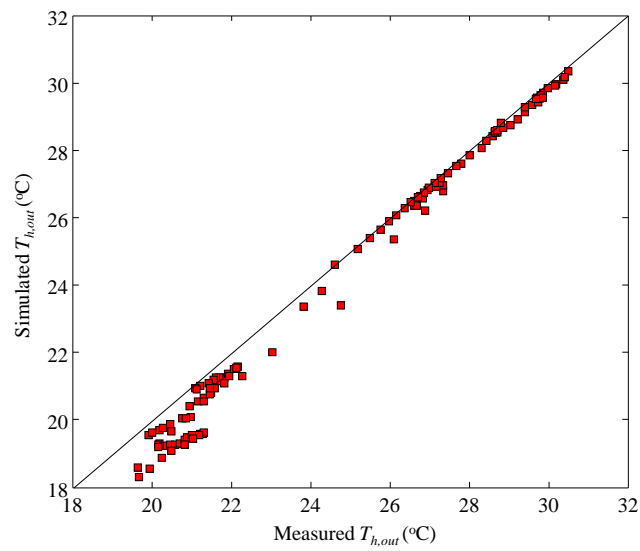


379

380

(b)

381



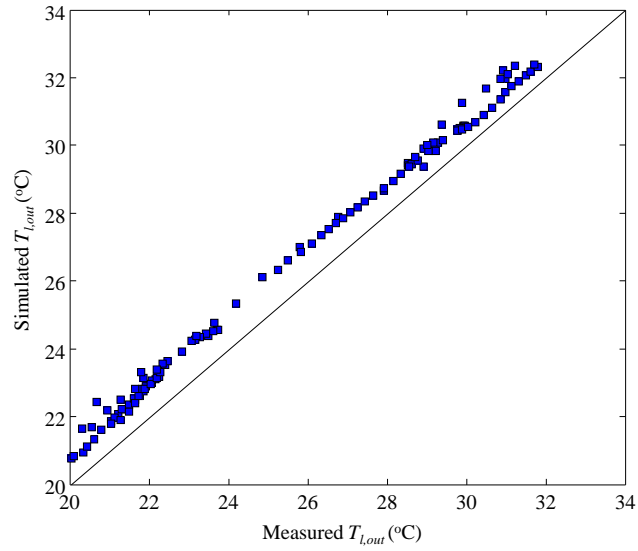
382

383

(c)

384





385

386

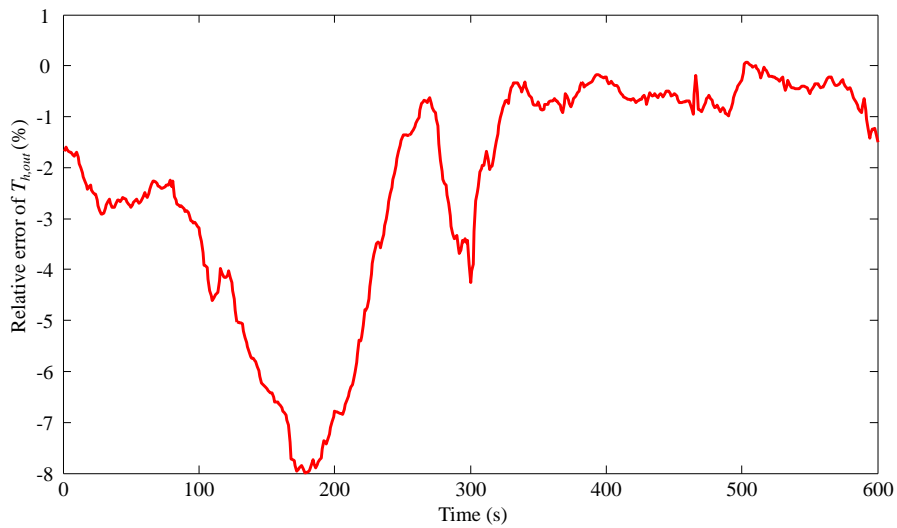
(d)

387 Fig. 11. Comparison of the measured and simulated outlet temperatures using parameters and

388 measured data provided in Ref. [16]. (a) Outlet temperature of high temperature side. (b) Outlet

389 temperature of low temperature side. (c) Validation of  $T_{h,out}$ . (d) Validation of  $T_{l,out}$ .

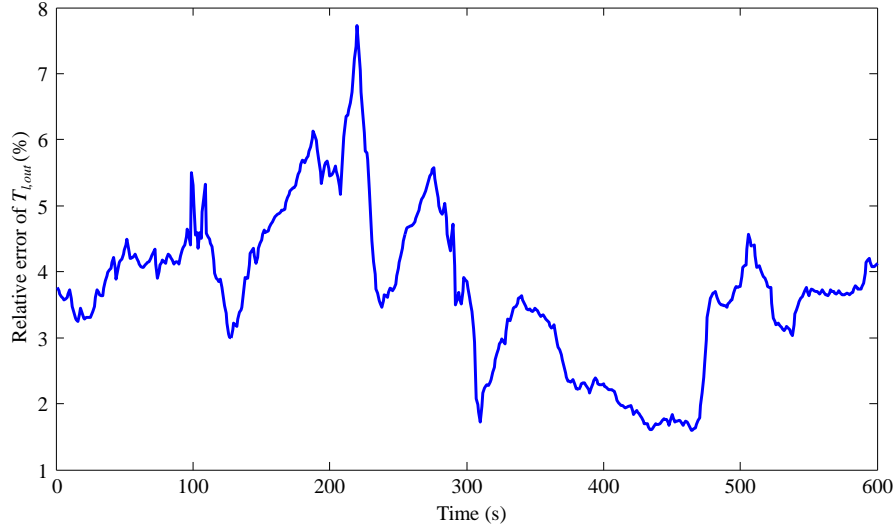
390



391

392

(a)



393

394

(b)

395 Fig. 12. Relative errors of the nonlinear model Eq. (5) and (6). (a) Relative error of  $T_{h,out}$ . (b)

396 Relative error of  $T_{l,out}$ .

397

### 398 5.2. Control and stability of heating substation

399 The nonlinear heating substation control system composed of plate heat

400 exchanger, equal percentage valve and PI controller was also established in Simulink

401 with the mathematical models Eq. (5), (6), (10) and (11). The dynamic responses of

402 the heating substation control system were calculated with Simulink. The parameters

403 of plate heat exchanger are listed in Table 1. The valve characteristic is shown in Fig.

404 6. The time delay of temperature sensor is  $\tau = 5s$ .

405

Description	Symbol	Value	Unit
channel width	$b$	0.8	m
channel length	$l$	1.36	m

water specific heat capacity	$c_p$	4220	kJ/(kg · K)
empirical parameters	$C$	0.64	/
distance between neighboring plates	$d$	4.5	mm
plate thickness	$d_p$	0.5	mm
number of flow channels in each side	$M$	137	/
empirical parameters	$n_1$	0.23	/
empirical parameters	$n_1$	0.75	/
water density	$\rho$	970	kg/m <sup>3</sup>
thermal conductivity of high temperature side water	$\lambda_h$	0.68	W/(m K)
thermal conductivity of low temperature side water	$\lambda_l$	0.67	W/(m K)
thermal conductivity of plate	$\lambda_p$	15	W/(m · K)
dynamic viscosity of high temperature side water	$\mu_h$	0.00028	Pa · m
dynamic viscosity of low temperature side water	$\mu_l$	0.00041	Pa · m

406 Table 1. Parameters of plate heat exchanger

407 In this section, the operation stability of heating substation was studied. The  
408 controller was tuned with the frequency domain approach [12]. In order to illustrate  
409 that if the controller is tuned and works well under low primary supply temperature  
410 condition, the operation stability may not be ensured at high primary supply  
411 temperature, dynamic performances of heating substation under low and high primary  
412 supply temperatures with the PI controller tuned at low supply temperature were  
413 studied.

#### 414 5.2.1. Dynamic responses in low primary supply temperature

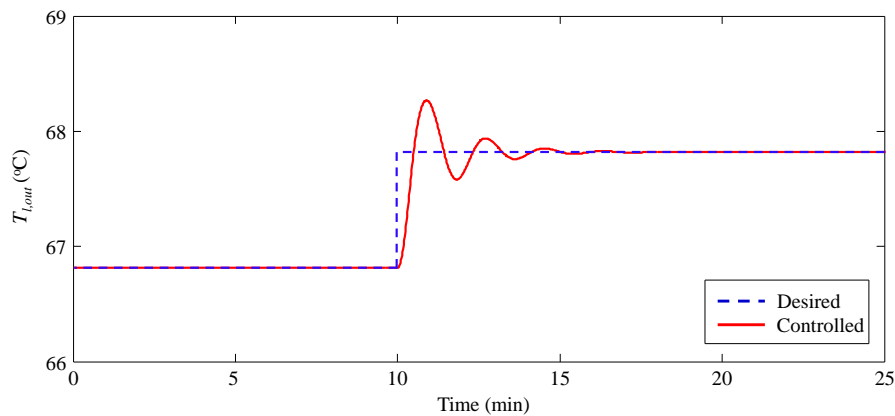
415 The PI controller is usually tuned under a certain operating condition. For the  
416 case study in this subsection, the following low primary supply temperature operating  
417 condition is chosen for controller tuning:  $T_{l,in} = 40$  °C,  $T_{h,in} = 70$  °C,  $q_l = 0.03$

418  $\text{m}^3/\text{s}$ . The PI controller is tuned by simulating the reference tracking response of  
 419  $T_{l,out}$  around the operating condition. The PI controller is tuned as:

$$420 \quad K_1 = 0.004 \frac{s+1}{s} \quad (14)$$

421 The dynamic responses of heating substation control system were calculated with the  
 422 nonlinear Simulink model.

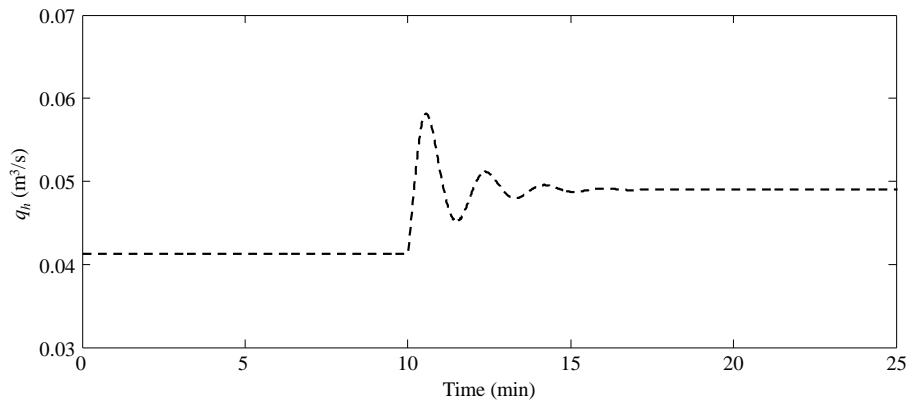
423 Fig. 13 shows the reference tracking responses under the control of  $K_1$ . When  
 424 the desired secondary supply temperature  $T_{l,out}$  changes from 66.8 °C to 67.8 °C, the  
 425 controlled  $T_{l,out}$  tracks the new value in about 5 minutes and the overshoot is less  
 426 than 0.5 °C. Fig. 14, Fig. 15 and Fig. 16 show the disturbance rejection responses to  
 427 step variations of  $T_{h,in}$ ,  $T_{l,in}$  and  $q_l$ , respectively. Fig. 14 shows that when primary  
 428 supply temperature  $T_{h,in}$  changes from 70 °C to 71 °C, the deviation of secondary  
 429 supply temperature  $T_{l,out}$  from the desired value can be controlled within 1 °C. Fig.  
 430 15 shows that if secondary return temperature changes from 40 °C to 35 °C, the  
 431 deviation of  $T_{l,out}$  from desired value can be restricted within 0.5 °C. Fig. 16 shows  
 432 that when the secondary flow rate  $q_l$  varies from 0.03  $\text{m}^3/\text{s}$  to 0.04  $\text{m}^3/\text{s}$ , the  
 433 deviation of  $T_{l,out}$  from desired value is within 2 °C.



434

435

(a)



436

437

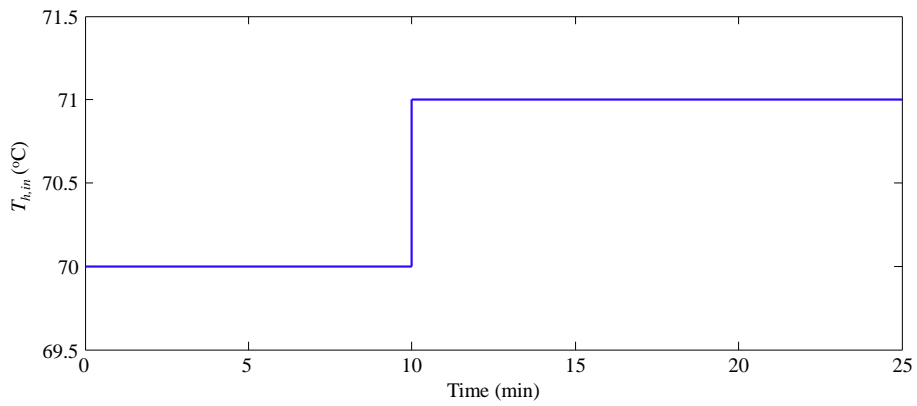
(b)

438 Fig. 13. System responses for tracking desired  $T_{l,o}$  under the control of controller  $K_1$  (with

439  $T_{l,in} = 40$  °C,  $T_{h,in} = 70$  °C,  $q_l = 0.03$  m<sup>3</sup>/s.). (a) Tracking response of  $T_{l,o}$ . (b) Tracking

440 response of  $q_h$ .

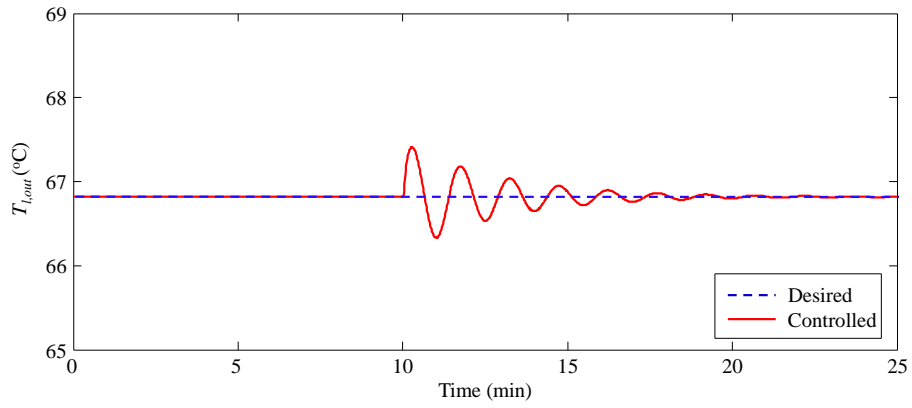
441



442

443

(a)

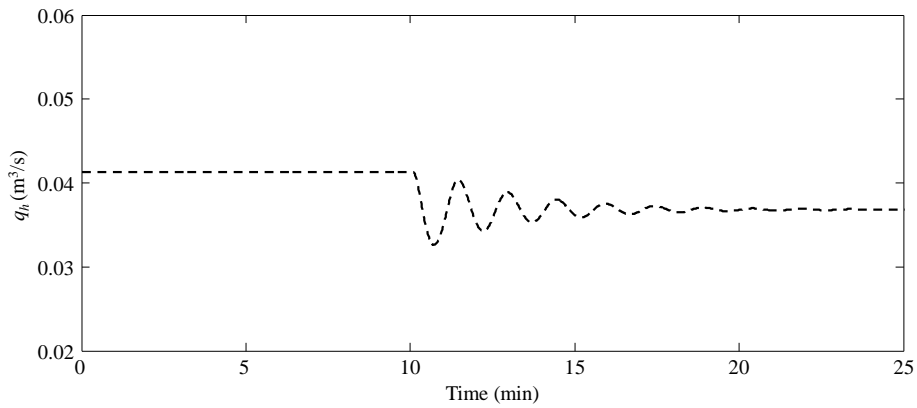


444

445

(b)

446



447

448

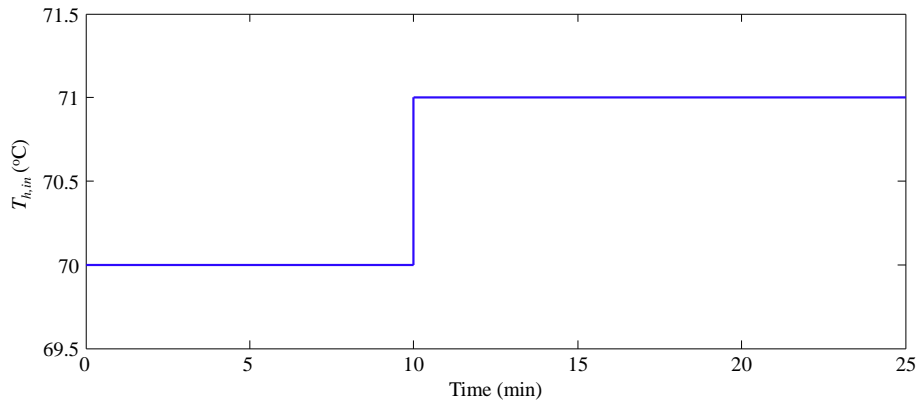
(c)

449 Fig. 14. System responses for rejecting the variation of  $T_{h,in}$  under the control of  $K_1$  (with

450  $T_{l,in} = 40$  °C,  $q_l = 0.03$  m<sup>3</sup>/s and desired  $T_{l,out} = 66.8$  °C). (a) Variation of  $T_{h,in}$ . (b)

451 Response of controlled  $T_{l,out}$ . (c) Response of  $q_h$ .

452

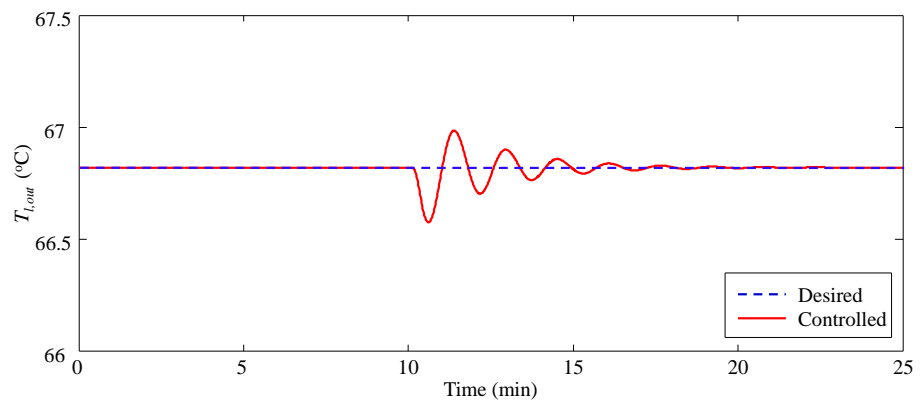


453

454

(a)

455

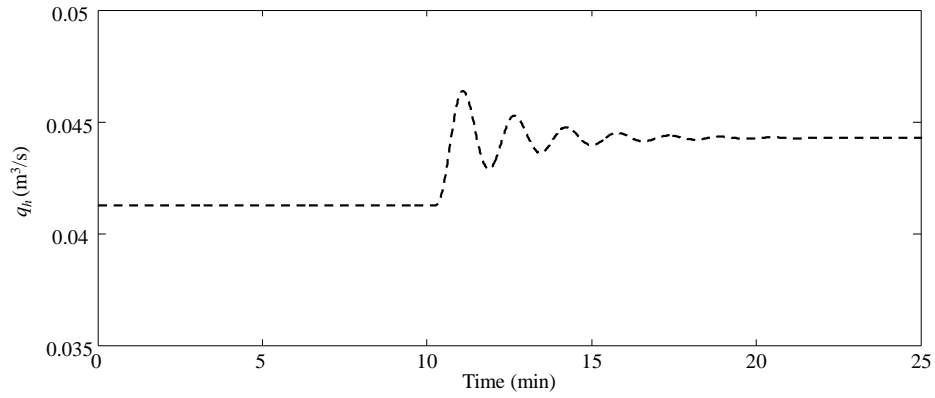


456

457

(b)

458



459

460

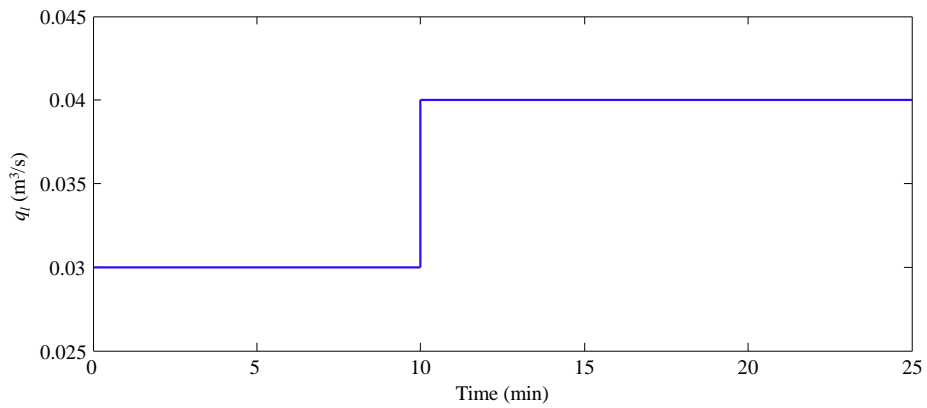
(c)

461 Fig. 15. System responses for rejecting the variation of  $T_{l,in}$  under the control of  $K_1$  (with

462  $T_{h,in} = 70$  °C,  $q_l = 0.03$  m<sup>3</sup>/s and the desired  $T_{l,out} = 66.8$  °C). (a) Variation of  $T_{l,in}$ . (b)

463 Response of controlled  $T_{l,out}$ . (c) Response of  $q_l$ .

464



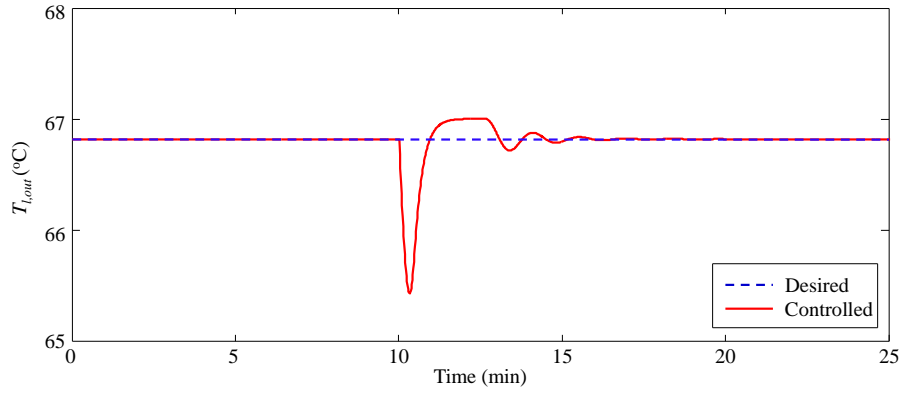
465

466

(a)

467



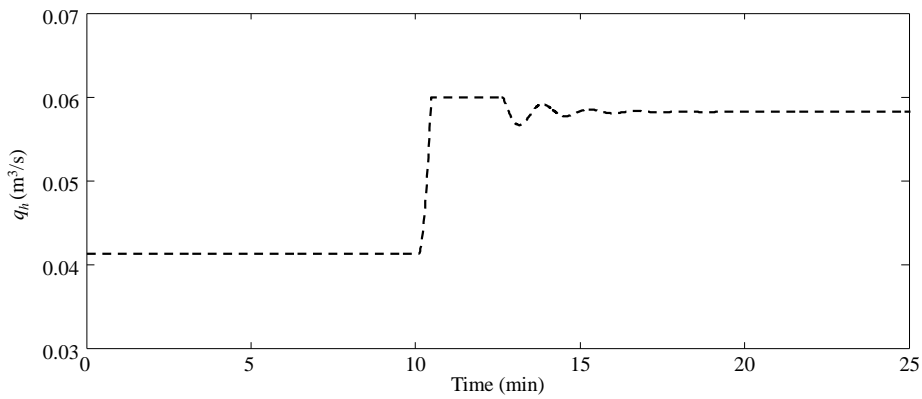


468

469

(b)

470



471

472

(c)

473 Fig. 16. System responses for rejecting the variation of  $q_l$  under the control of  $K_1$  (with  $T_{h,in} =$

474  $70\text{ }^\circ\text{C}$ ,  $T_{l,in} = 40\text{ }^\circ\text{C}$  and desired  $T_{l,out} = 66.8\text{ }^\circ\text{C}$ ). (a) Variation of  $q_l$ . (b) Response of

475 controlled  $T_{l,out}$ . (c) Response of  $q_h$ .

476 These reference tracking and disturbance rejection responses indicate that under

477 the control of  $K_1$ , the heating substation system is stable around the operating

478 condition of  $T_{h,in} = 70\text{ }^\circ\text{C}$ ,  $T_{l,in} = 40\text{ }^\circ\text{C}$ ,  $q_l = 0.03\text{ m}^3/\text{s}$ . Hence, the tuned PI

479 controller  $K_1$  seems to be suitable for the control of the heating substation with the

480 proposed parameters. However, the simulation test of responses is only conducted  
481 around the operating condition of  $T_{h,in} = 70$  °C,  $T_{l,in} = 40$  °C,  $q_l = 0.03$  m<sup>3</sup>/s. When  
482 the operating condition changes largely, instability may occur as the measured data  
483 shown in Fig. 3.

484

### 485 5.2.2. Robust stability test and retuning of the controller

486 In order to investigate the stability of the heating substation under the control of  
487 controller  $K_1$ , the stability criterion proposed in subsection 4.3 was adopted. Fig.  
488 17-(a) shows the Nyquist curves of the heating substation under the control of  $K_1$  at  
489 all possible operating conditions. The possible operating conditions were defined as  
490 conditions that satisfy:  $65$  °C  $\leq T_{h,in} \leq 95$  °C,  $30$  °C  $\leq T_{l,in} \leq 50$  °C,  $0.01$  m<sup>3</sup>/s  $\leq$   
491  $q_h \leq 0.06$  m<sup>3</sup>/s and  $0.03$  m<sup>3</sup>/s  $\leq q_h \leq 0.04$  m<sup>3</sup>/s. This range can cover most of the  
492 operation conditions of the heating substation proposed in this paper. The proposed  
493 method in section 4.3 can be used to study the operation stability at these possible  
494 operating condition.

495 As is shown, the black curve, which denotes the Nyquist curve of the  $T_{h,in} = 70$   
496 °C,  $T_{l,in} = 40$  °C,  $q_l = 0.03$  m<sup>3</sup>/s condition, does not encircle or cross the point (-1,  
497 0). This is the reason that the heating substation operates stably under the control of  
498  $K_1$  around the condition of  $T_{h,in} = 70$  °C,  $T_{l,in} = 40$  °C,  $q_l = 0.03$  m<sup>3</sup>/s. However,  
499 there are still many cases don't satisfy this criterion. This means that the heating  
500 substation will be unstable under the control of  $K_1$  in some operating conditions. Fig.  
501 18-(a) shows the variation of  $T_{h,in}$  and desired  $T_{l,out}$ , which will lead to instability

502 of the heating substation (with  $T_{l,in} = 40$  °C,  $q_l = 0.03$  m<sup>3</sup>/s). As is shown in Fig.  
503 18-(b) and 18-(c), the dynamic responses of  $T_{l,out}$  and  $q_h$  under the control of  $K_1$   
504 (drawn in dark blue) become oscillatory when the primary supply temperature  $T_{h,in}$   
505 increases from 70 °C to 85 °C. The oscillation form of the primary flow rate  $q_h$ ,  
506 shown in Fig. 18-(b), is very similar to the measured primary flow rate data shown in  
507 Fig. 3-(a). The heating substation becomes unstable because the increase of primary  
508 supply temperature  $T_{h,in}$  makes the loop gain  $|L(i\omega)|$  larger and causes the curve of  
509  $L(i\omega)$  to encircle point (-1, 0). This phenomenon also indicates that the high primary  
510 supply temperature conditions are worse than low supply temperature conditions. This  
511 also demonstrates that controllers tuned at a certain operating condition cannot ensure  
512 stability for all operating conditions.

513 In order to stabilize the heating substation, controller  $K_1$  should be tuned again  
514 by considering all the possible operating conditions. The red Nyquist curve in Fig.  
515 17-(a) denotes the worst operation condition. If the worst condition Nyquist curve  
516 doesn't encircle or cross the point (-1, 0), the heating substation will be stable at all  
517 operating condition. Therefore, according to Fig. 17-(a), to make the red curve do not  
518 encircle or cross the point (-1, 0), the controller gain  $k_c$  should be smaller. Fig. 17-(b)  
519 shows the Nyquist curves of the heating substation under the control of  $K_2$  at all  
520 possible operating conditions, where

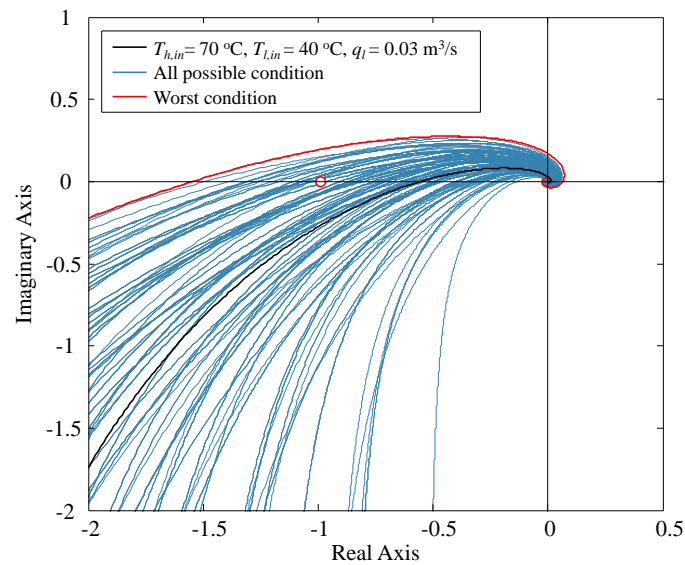
$$521 \quad K_2 = 0.002 \frac{s+1}{s}$$

522 (18)

523 As is shown in Fig. 17-(b), the Nyquist curves of all the possible conditions do not

524 encircle or cross the point (-1, 0). Therefore the heating substation under the control  
 525 of controller  $K_2$  will be stable even in worse condition. In Fig. 18-(b) and Fig. 18-(c),  
 526 the responses drawn in red are under the control of  $K_2$ . As is shown, the operation of  
 527 heating substation remains stable even when primary supply temperature increases to  
 528 very high.

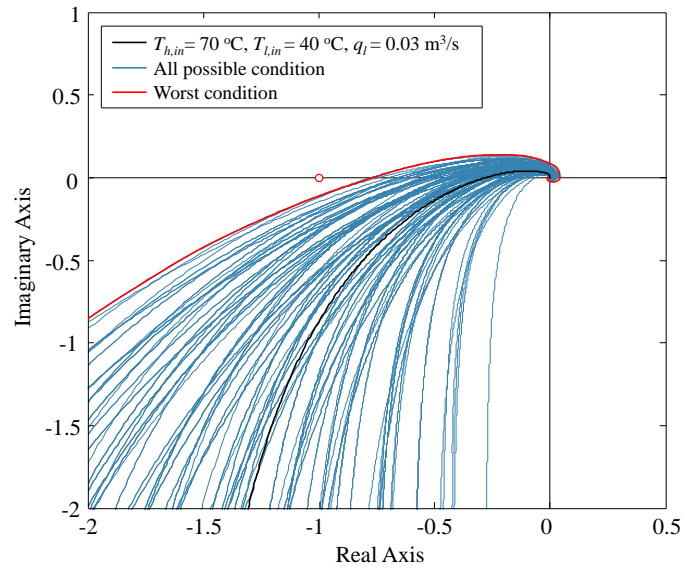
529 Hence, the heating substation controller tuned at certain operating conditions  
 530 may be unstable when operating condition changes in large range. To ensure operation  
 531 stability of heating substation at all conditions, the operation stability should be tested  
 532 when operating condition changes, and the proposed method can be used as a tool for  
 533 analyzing the operation stability of heating substation at all possible operating  
 534 conditions.



535

536

(a)



537

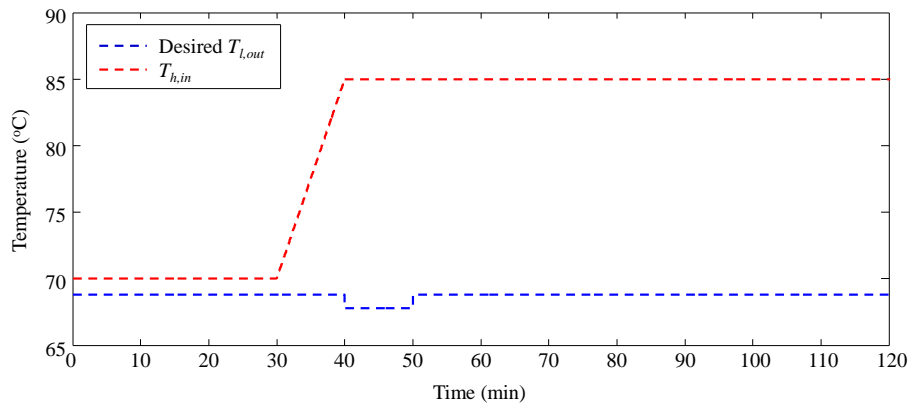
538

(b)

539 Fig. 17. Nyquist curves of heating substation system at all possible operating conditions. (a) Under

540 the control of  $K_1$ . (b) Under the control of  $K_2$ .

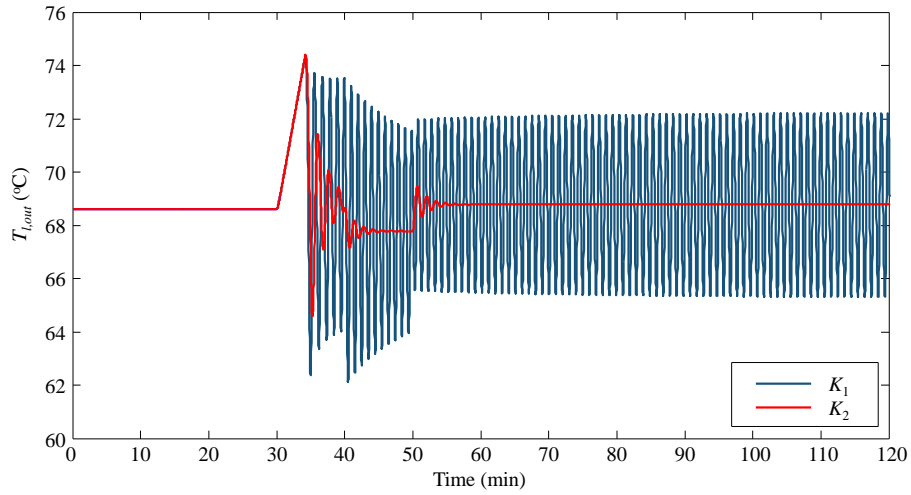
541



542

543

(a)

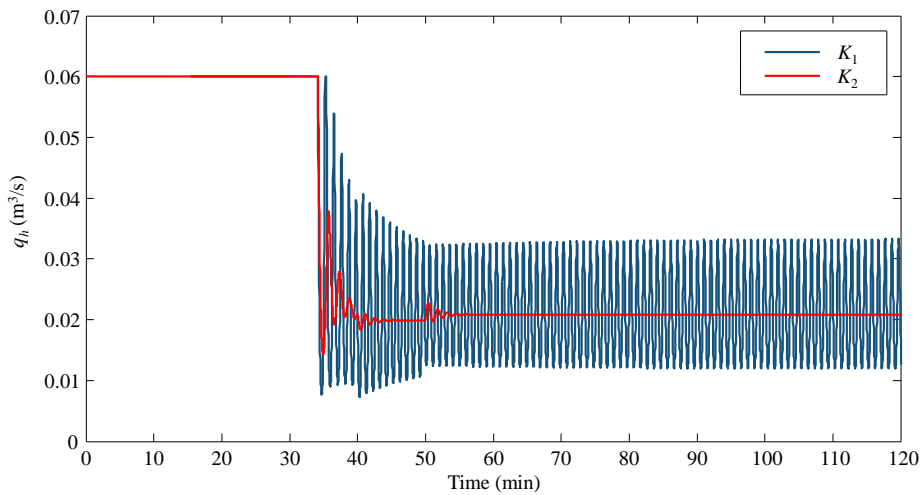


544

545

(b)

546



547

548

(c)

549 Fig. 18. Dynamic responses in worse operating condition under the control of  $K_1$  and  $K_2$  (with

550  $T_{l,in} = 40$  °C,  $q_l = 0.03$  m<sup>3</sup>/s). (a) Variation of desired  $T_{l,out}$  and  $T_{h,in}$ . (b) Responses of  $q_h$ . (c)

551 Responses of controlled  $T_{l,out}$ .

552

553 **6. Conclusions**

554 In this paper, the nonlinear ODE model of plate heat exchanger was developed.  
555 Based on the nonlinear ODE model, the linearized model of plate heat exchanger for  
556 controller design and stability analysis was derived. The nonlinear ODE model of  
557 plate heat exchanger was solved with Simulink. In order to validate the nonlinear  
558 plate heat exchanger model, the parameters and measured data provided in Ref. [16]  
559 were adopted in simulation. The simulated results were compared with the measured  
560 data provided in the literature. Associated with the equal percentage valve model and  
561 controller model, the Nyquist stability criterion was proposed for analyzing the  
562 operation stability criterion of district heating substation at all operating conditions.  
563 The dynamic responses of heating substation under the control of a PI controller tuned  
564 at a certain operating condition were analyzed. And the operation stability of heating  
565 substation was also studied. And the following conclusions have been drawn:

566 (1) Comparison of the measured data and simulated results of the plate heat  
567 exchanger shows that the proposed nonlinear ODE model has satisfactory  
568 accuracy in describing the thermal dynamics of plate heat exchanger. Relative  
569 errors of the two outlet temperatures:  $T_{h,out}$  and  $T_{l,out}$  are both varying within  
570  $\pm 8\%$ .

571 (2) Simulation results of heating substation control system indicate that the controller  
572 tuned at a certain operating condition may be unstable, when operating condition  
573 changes in large range. For example, the operation instability of district heating  
574 substation may occur at the high primary supply temperature, if the controller is  
575 tuned at low primary supply temperature.

576 (3) With the proposed stability criterion for heating substation operation, the  
 577 controller can be retuned to be stable at all operating conditions.

578 Since operation stability of heating substation is the basic requirement of the  
 579 operation and is of great importance to energy conservation of pumping system,  
 580 reducing the failure rate of control valve and improving the heating quality of the  
 581 secondary system, the proposed method will be very helpful and applicable to heating  
 582 substation controller tuning and operation stability analysis for stable operation.

583

#### 584 **Appendix A. Calculation of heat transfer coefficient $k$**

585 The overall heat transfer coefficient of plate heat exchanger can be determined  
 586 by the following formula:

$$587 \quad k = \left( \frac{1}{k_h} + \frac{1}{k_p} + \frac{1}{k_l} \right)^{-1} \quad (\text{A-1})$$

588 where  $k_p = \frac{\lambda_p}{d_p}$  is the heat transfer coefficient of the plate.  $k_h$  and  $k_l$  are

589 determined by the following formulas [16]:

$$590 \quad k_h = \frac{Nu_h \lambda_h}{D}, \quad Nu_h = C_{Nu} \cdot Re_h^{n_1} \cdot Pr_h^{n_2}, \quad Re_h = \frac{\rho D q_h}{\mu_h M b d}, \quad Pr_h = \frac{\mu_h c_p}{\lambda_h} \quad (\text{A-2})$$

$$591 \quad k_l = \frac{Nu_l \lambda_l}{D}, \quad Nu_l = C_{Nu} \cdot Re_l^{n_1} \cdot Pr_l^{n_2}, \quad Re_l = \frac{\rho D q_l}{\mu_l M b d}, \quad Pr_l = \frac{\mu_l c_p}{\lambda_l} \quad (\text{A-3})$$

592 where  $D = 2d$  is the hydraulic diameter;  $\lambda_h$  and  $\lambda_l$  are the heat conductivities of  
 593 the high temperature side water and the low temperature side water, respectively;

594  $Nu_h$  and  $Nu_l$  are the Nusselt numbers of the two sides;  $C_{Nu}$ ,  $n_1$  and  $n_2$  are  
 595 empirical parameters provided by the manufacturer;  $Re_h$  and  $Re_l$  are the Reynolds

596 numbers of the two sides;  $Pr_h$  and  $Pr_l$  are the Prandtl numbers of the two sides;  $\mu_h$

597 and  $\mu_l$  are the dynamic viscosities of the two sides.





616  $C = (O_{1 \times N}, O_{1 \times (N-1)}, 1)$

617 where  $A_{11}$ ,  $A_{12}$ ,  $A_{21}$  and  $A_{22}$  are  $N \times N$  matrices.  $T$ ,  $B_1$ ,  $B_2$ ,  $B_3$  and  $B_4$  are  
618  $2N$ -dimensional vectors.

619 The transfer function form of the linearized plate heat exchanger model is:

620  $T_{l,out} = G(s)q_h + G_{d,1}(s)q_l + G_{d,2}(s)T_{h,in} + G_{d,3}(s)T_{l,in}$

621 where

622  $G(s) = C(sI - A)^{-1}B_1$

623  $G_{d,1}(s) = C(sI - A)^{-1}B_2$

624  $G_{d,2}(s) = C(sI - A)^{-1}B_3$

625  $G_{d,3}(s) = C(sI - A)^{-1}B_4$

626

627

## 628 **Acknowledgement**

629 This work was supported by the State Oceanic Administration of China (Grant  
630 No. cxsf-43); and the National Natural Science Foundation of China (No. 51106110).

631

## 632 **Reference**

633

634 [1] Building energy conservation research center of Tsinghua University, The annual  
635 development research report of China building energy conservation, 2015 ed.,  
636 Building Industry Press, Beijing, 2015. (in Chinese)

637 [2] J. Gustafsson, J. Delsing, J.V. Deventer, Improved district heating substation  
638 efficiency with a new control strategy, Appl. Energy 87(2010) 1996-2004.

- 639 [3] J. Gustafsson, J. Delsing, J. V. Deventer, Experimental evaluation of radiator  
640 control based on primary supply temperature for district heating substations, *Appl.*  
641 *Energy* 88(2011) 4945-4951.
- 642 [4] H. Gadd, S. Werner, Achieving low return temperatures from district heating  
643 substations, *Appl. Energy* 136(2014) 59–67.
- 644 [5] H. Gadd, S. Werner, Fault detection in district heating substations, *Appl. Energy*  
645 157(2015) 51-59.
- 646 [6] M. Brand, J.E. Thorsen, S. Svendsen, Numerical modelling and experimental  
647 measurements for a low-temperature district heating substation for instantaneous  
648 preparation of DHW with respect to service pipes, *Energy* 41(2012) 392-400.
- 649 [7] M. Brand, A.D. Rosa, S. Svendsen, Energy-efficient and cost-effective in-house  
650 substations bypass for improving thermal and DHW (domestic hot water) comfort in  
651 bathrooms in low-energy buildings supplied by low-temperature district heating,  
652 *Energy* 67(2014) 256-267.
- 653 [8] M. Kuosa, M. Aalto, M.E.H. Assad, et al., Study of a district heating system with  
654 the ring network technology and plate heat exchangers in a consumer substation,  
655 *Energy Build.* 80(2014) 276–289.
- 656 [9] L. Dobos, J. Abonyi, Controller tuning of district heating networks using  
657 experiment design techniques, *Energy* 36(2011) 4633-4639.
- 658 [10] S.K. Al-Dawery, A.M. Alrahawi, K.M. Al-Zobai Dynamic modeling and control  
659 of plate heat exchanger, *Int. J. Heat Mass Tran.*, 55(2012) 6873-6880.
- 660 [11] A. Michel, A. Kugi, Model based control of compact heat exchangers  
661 independent of the heat transfer behavior, *J. Process Contr.*, 24(2014)286-298.
- 662 [12] G.F. Franklin, D.J. Powell, A. Emami-Naeini, *Feedback Control of Dynamic*  
663 *Systems*, seventh ed., Pearson, New York, 2015.

- 664 [13] P. Andersen, T.S. Pedersen, J. Stoustrup, et al., Proceedings of the 2000 American  
665 Control Conference. ACC (IEEE Cat. No.00CH36334), Chicago, IL, 2000, pp.  
666 135-139 vol.1.
- 667 [14] Tahersima F, Stoustrup J, Rasmussen H. An analytical solution for  
668 stability-performance dilemma of hydronic radiators, Energy Build. 64(2013)  
669 439-446.
- 670 [15] Y. Wang, S. You, X. Zheng, H. Zhang, Accurate model reduction and control of  
671 radiator for performance enhancement of room heating system, Energy Build  
672 138(2017) 415-431.
- 673 [16] A. Michel, A. Kugi, Accurate low-order dynamic model of a compact plate heat  
674 exchanger, Int. J. Heat Mass Tran. 61(2013) 323-331.
- 675 [17] S. Skogestad, I. Postlethwaite, Multivariable Feedback Control: Analysis and  
676 Design, second ed., Wiley, New York, 2007.
- 677 [18] American Society of Heating, Air-Conditioning Engineers, ASHRAE handbook:  
678 heating, ventilating, and air-conditioning systems and equipment, SI ed; 2012.

679

680

681

682

683

684